Bioprocess and Biosystems Engineering (2018) 41:313–329
https://doi.org/10.1007/s00449-017-1878-8

CRITICAL REVIEW

Quantitative analysis of hydrogen peroxide with special emphasis on biosensors

Chandra S. Pundir[1] · Ritu Deswal[2] · Vinay Narwal[1]

Received: 11 August 2017 / Accepted: 7 December 2017 / Published online: 19 December 2017
© Springer-Verlag GmbH Germany, part of Springer Nature 2017

Abstract

Determination of hydrogen peroxide (H_2O_2) has become essential in pharmaceutical, biological, clinical and environmental studies. The conventional detection methods of H_2O_2 such as colourimetry, titration, chromatography, spectrophotometry, fluorimetry, chemiluminescence have limited success, due to their poor selectivity and sensitivity, long analysis time and lack of long-term reliability and reproducibility. The biosensors overcome these limitations because of their simplicity, rapidity, selectivity and high sensitivity. This review describes the principle, analytic parameters, merits and demerits of various methods of H_2O_2 determination with special emphasis on biosensors. The classification of biosensors based on various materials/nanomaterials and electrodes have been described in detail. The recent advances in vivo sensing and bio-sensing of H_2O_2 by hemoglobin nanoparticles are also presented. The significant challenges and future perspective for highly selective H_2O_2 detection are discussed.

Keywords Hydrogen peroxide · Biosensors · Nanomaterials · Biological materials

Introduction

Hydrogen peroxide (H_2O_2) is one of the most important substrate in various biological reactions catalyzed by multifunctional oxidases [1]. H_2O_2 (Mr-4.014 g/mol) is a strong oxidant with a skew, chain non-planar structure (Fig. 1). H_2O_2 exhibits several important properties such as oxidizing property, source of energy, gas formation on decomposition, source of free radicals, effects on biological processes and its use in chemical synthesis. Depending on exposure index (> 10%), H_2O_2 is an irritant to skin, eye, gastrointestinal tract, brain and mucous membrane. Accurate determination of H_2O_2 is highly important in the fields of biological, pharmaceutical, clinical and environment sciences, food processing and textile [2]. In industrial and medical areas, it is used for wastewater treatment, bleaching and sterilization. Besides cell cytotoxicity and anti-oxidation, H_2O_2 plays a key role as secondary messenger, modulating vital and complex biological pathways, namely cell growth, cell differentiation, apoptosis, vascular remodeling, immune activation, stomatal movement and root growth [3]. Elevated levels of H_2O_2 have been implicated as an etiological agent in multiple disease conditions including cancer, arthritis, diabetes, neurodegenerative disorders, cardiovascular diseases, asthma, ageing and oxidative stress-related diseases [4, 5]. Table 1 summarizes the various physico-chemical properties of H_2O_2. The detection of H_2O_2 sets the foundation for many analytical techniques and commercial test-kits such as colourimetry, fluorimetry, spectrophotometry, chemiluminescence and electrochemical method [6]. The first four techniques have obvious drawbacks, as these are time-consuming, expensive, require long pre-treatments for preparation of the samples, utilization of expensive reagent and interference [7], Among these methodologies, electro-chemical methods provides a convenient way for H_2O_2 determination, because of its easy fabrication, low cost of instrumentation, intrinsic sensitivity, high selectivity, and suitability for detecting and quantifying analytes in real-time [8]. In electrochemistry, H_2O_2 can be directly reduced/oxidized onto solid electrode surfaces. The detection of H_2O_2 with conventional noble metal electrodes is restricted by high over potential leading to slow electrode

✉ Chandra S. Pundir
pundircs@rediffmail.com

[1] Department of Biochemistry, Maharshi Dayanad University, Rohtak, Haryana 124001, India

[2] Centre for Medical Biotechnology, Maharshi Dayanad University, Rohtak, Haryana 124001, India

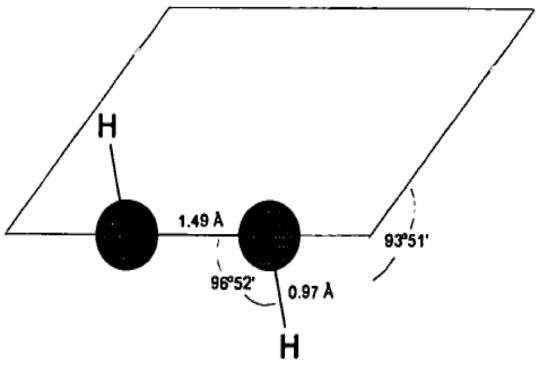

Fig. 1 Structure of hydrogen peroxide

kinetics and biofouling, causing interference of other co-existing electroactive species, which downgrade the sensing of real samples [9]. In these studies, conducting research on H_2O_2 detection was focused mainly on electrode modifications to solve the problem of low sensitivity and high over potentials. To fabricate selective H_2O_2 biosensor, platinum nanoparticles, redox polymers, metal oxides, nanofibres, carbon nanotube, a large number of advanced nanomaterials viz carboxylic acid nano-hybrids, fluorophores, graphene capsules, reduced graphene oxide, tetraethyl orthosilicate, polydimethylsiloxane and TTF-modified graphite disc electrodes were used [10]. The present review is aimed to gain an insight into the recent advances in detailed analysis (construction and performance) of the H_2O_2 biosensors over conventional analytical methods for H_2O_2 determination.

Conventional methods for determination of H_2O_2

The conventional methods for detection of H_2O_2 can be classified into different categories:

Titrimetry

It is used to calculate unknown amount of H_2O_2 in an identified sample of known concentration. Titrimetric procedures employed iodometry, permanganate and cerium (IV) in acidic media. Klassen et al. [11] estimated 300 µM H_2O_2 using I_3^- method, after calibrating with permanganate. ε_{max} was also measured at 351 nm as 25 800 M^{-1} cm^{-1} from calibration plot of the I_3^- method against prepared by titration with potassium dichromate ($KMnO_4$) [11]. Murty et al. 1981 determined H_2O_2 potentiometrically within a medium containing 8–11 M phosphoric acid [12]. Kieber and Helz used a modified version of the iodometric titration in water matrices, where iodine was liberated as follows: $H_2O_2 + 2H^+ + 2I^- = I_2 + 2H_2O$. I_2 produced was consumed by adding excess of phenylarsine oxide. To obtain end result, remaining volume of phenylarsine oxide was titrated with I_2 [13].

$$I_2 + (2)H_2O + C_6H_5AsO = 2I^- + 2H^+ + C_6H_5AsO(OH)_2.$$

The end point was determined, when the intense blue colour of the starch–iodine complex was disappeared. The limit of detection limit (LOD) was 0.02 µM. Another high-throughput two-step absorbance microtitre plate method was developed, titrating an acidified H_2O_2 solution with standard

Table 1 Physiochemical properties H_2O_2

IUPAC name	Hydrogen peroxide
Appearance	Colorless liquid
Molecular formula	H_2O_2
Molecular mass	34.014 g/mol
Solubility	Miscible with water; sol in ether; insol in petroleum ether
Stability	A very unstable compound that breaks down readily
Melting point	− 40 °C
Boiling point	152 °C
Density	1.4425
Viscosity	1.245 centipoises
Vapor pressure	1.97 mm Hg
pH	Weak acid
pK_a	11.75
Ionization potential	10.54 eV
Index of refraction	1.4061@28 ℃
Surface tension	80.4 dynes/cm
Therapeutic uses	Anti-septic agents, disinfectant, oxidants, bleaching, microbiocide
Biofluid location	Blood

cerium (IV) sulfate. Cerium (IV) sulfate gets converted into cerium (III) sulfate and potassium iodide into iodine [14].

Merits Simple to perform, cost effective and one of the most commonly used method.

Demerits Time consuming, requirement of moderate skill and practice for effective results and proper calibration of the instrument but not accurate at low concentrations.

Spectroscopy

The simplest and most widely available instrumental technique for determination of H_2O_2, generally involves the formation of colored compounds for subsequent absorbance measurements. A method comparing the reaction of methyl blue and toluidine blue with iodine solution was introduced for determination of H_2O_2 based on the following reaction:

$$H_2O_2 + 2KI + 2HCl \rightarrow I_2(aq) + 2KCl + 2H_2O.$$

Methyl blue reaction yielded a single-peak visible spectrum with higher extinction coefficient, $M^{-1}\ cm^{-1} = 49{,}100$ [15]. Matsubara et al. demonstrated the use of mixture of titanium IV and 2,4((5-bromopyridyl)azo)5-(N propyl-*N*-sulfopropyl amino) phenol disodium for H_2O_2 determination [16]. The molar absorptivity was $5.710^4\ M^{-1}\ cm^{-1}$ at 539 nm wavelengths. Clapp et al. developed a method to measure H_2O_2 selectively in aqueous solution with titanium (IV) sulphate, yielding a yellow peroxotitanium species at 407 nm [17]. A rapid, reproducible and sensitive method was developed to detect in vitro H_2O_2 activity by 1,10-phenanthroline method [18]. A study reported catalytic decomposition of H_2O_2 by monomeric molybdenum (VI). Hydroquinone, ammonium molybdate, and anilinium sulphate with different H_2O_2 concentrations was mixed and absorbance was determined at 550 nm [19]. Zhang and Wong estimated concentration of H_2O_2 in marine water in the presence of horseradish peroxidase at 592 nm at pH 4.0 by leuco crystal violet oxidation (LCV). LOD was 20 nM with ± 1% precision [20]. A method based on the hydroxylation of phenol was introduced to measure H_2O_2 in water and rainwater samples. The reaction involved presence of iron (II) ions in dilute sulfuric acid medium. The product possessed two bands with maximum absorption at 245 and 300 nm. Linear calibration curve was obtained in 2.0×10^{-7} to 3.0×10^{-4} mol/L range with LOD 9.5×10^{-8} mol L^{-1} [21]. Huang et al. introduced a rapid and reproducible method for H_2O_2 determination using 4AAP-DEA-βCD-hemin [22]. The LOD obtained through this method was 8.4×10^{-5} with molar absorption coefficient 1.65×10^4 mol/L/cm. A simple and accurate method for the determination of H_2O_2 in pulp bleaching effluents was introduced in 2013 by Zhang et al. [23]. In this method, H_2O_2 reacted with vanadium pentoxide in H_2SO_4 solution forming a red brown peroxovanadate complex.

Merit These methods exhibit simple and fast analysis.

Demerit They showed analytical interference, slow color development, and low specificity.

Colorimetry

Determination of H_2O_2 by iodide and starch was first reported by Eisenberg in 1943. Color intensities of H_2O_2 sample solutions treated with titanium sulfate reagent was measured. The chemical reaction was as follows: $Ti^{++++} + H_2O_2 + 2H_2O = H_2TiO_4 + 4H^+$.

Formation of pertitanic acid results in formation of yellow color permitting 0.2–3.0 mg/100 ml determination of H_2O_2 concentrations [24]. A sensitive colorimetric method based on iodide oxidation in the presence of $(NH4)_2MoO_4$ (ammonium molybdate) for direct determination of H_2O_2 in micromolar quantities was reported. Molar absorptivity of the starch–iodine complex was 39.45 $mmol^{-1}cm^{-1}L$ at 570 nm [25]. Enzyme-based colorimetric method was optimized by Fernando and co-workers in 2015 for determination of H_2O_2 scavenging capacity in plant extracts. A significant pink-colored quinoneimine dye was formed when H_2O_2 reacts with phenol, 4-aminoantipyrine, horseradish peroxidase (HRP) in 0.4M phosphate buffer, pH 7.0 [26]. Optimized assay conditions were 30 min as reaction time, pH 7.0, 37 °C, 0.7 mM H_2O_2 concentration and 1 U/ml enzyme concentration. The reported values of limit of quantitation and limit of detection (LOD) were 411 and 136 mM, respectively. A simple and rapid method based on oxidation of phenol red was described for the measurement of H_2O_2 released by cells in tissue culture. A direct linear relationship between concentration of H_2O_2 ranging from 1 to 60 nmol/ml and absorbance at 520 nm was obtained [27]. A direct colorimetric method using 4-nitrophenyl boronic acid for rapid determination of H_2O_2 in aqueous media was developed. Nitrophenylboronic acid reacts with H_2O_2 to produce 4-nitrophenol. An LOD of ~ 1.0 µM was reported [28]. Nitinaivinij et al. proposed a highly sensitive colorimetric method for quantification of H_2O_2, based on chromaticity analysis of silver nanoprisms (AgNPrs). AgNPrs decomposition by H_2O_2 produced yellow color. The protocol recognized H_2O_2 concentration at 1.57 mM with good accuracy and reproducibility [29].

Merit No requirement of complicated apparatus and easy to perform.

Demerit Low sensitivity, false-positive readings, not applicable in turbid samples.

Chromatography

Takahashi reported a method for separating H_2O_2 by HPLC with electrochemical detector and cation-exchange resin gel column of sulphonated styrene divinyl benzene copolymer.

The linearity and LOD were 0.9984 and 0.2 pmol, respectively, [30]. H_2O_2 was separated isocratically by HPLC on octadecylsilyl column by Wada et al. in 2003. The LOD was 1.1 µM [31]. A gas-chromatographic method was developed for determination of H_2O_2 in oxidized butyric acid. The absorbance was measured at 517 nm [32]. H_2O_2 was separated by a ligand exchange type column in which a sulfonated polystyrene/divinyl benzene cation-exchange resin was packed [33]. Steinberg determinated H_2O_2 using reverse phase HPLC. The iodovanillic acid thus formed was detected by UV absorption at 280 nm providing ~ 0.1 µM LOD [34]. Gimeno et al. determined H_2O_2 quantitatively in 35 teeth and hair bleaching products by HPLC/UV plus ceric titrimetric method. This method quantified triphenylphosphine oxide (OPPh3) formed by oxidation of triphenylphosphine (PPh3) [35].

Merit Simple, low cost, choice of stationary phase and columns.

Demerit Expensive, require more skilled manpower, time consuming, interferences.

Chemiluminescence methods

Chemiluminescence (CL) is an important method for analysis and quantification of H_2O_2 in different samples. Numerous CL agents such as fluorescein, luminol, dioxetanes, oxalate and its derivatives and acridinium dyes were used as per their specificity. Segawa et al. proposed sensitive H_2O_2 analysis with fluorescein chemiluminescence using HRP as a catalyst. At pH 7.0, the optimum HRP and fluorescein concentrations were 5×10^8 and 6.6×10^4 molar, respectively [36]. A study proposed chemiluminescence detection of H_2O_2 concentrations in various water samples. The method was based on that H_2O_2 induced luminol oxidation in the presence of Co^{2+} ions. The experimental LOD for H_2O_2 was 3.04×10^{-4} and 6.25×10^{-5} M, respectively, making the assay suitable for determining micromolar amount of H_2O_2 [37]. An improved chemiluminescence method was developed based on cobalt (II)-catalysed luminol oxidation. This method has enhanced sensitivity towards micromolar determination of H_2O_2 by avoiding quenching effects [38].

Merit Simple to apply, easy to perform, reliable.

Demerit Requirement of complex instrumentation and prone to interferences.

Fluorescence methods

An accurate and simple phosphine-based fluorescent method was developed by Onoda et al. in 2003 to determine H_2O_2 in tissue fractions. Linear calibration curve was attained in the range of 12.5–500 ng H_2O_2 [39]. Paital in 2014 proposed a modified spectrofluorimetric method for determination of H_2O_2 using homovanillic acid oxidation. Biological samples were precipitated with 5% TCA and neutralized by K_2HPO_4 [40]. Chen et al. introduced a new sensitive fluorescent quenching method for H_2O_2 determination in rain water. At pH 3.09, a calibration graph was obtained between 5.0×10^{-7} to 9.0×10^{-4} mol/l [41].

Merit Multiple samples analysis, sensitive, more efficient and cost effective.

Demerit Requirement of sophisticated imaging techniques, false positives but not applicable for detection of non-fluorescence compounds.

Chemibioluminescence imaging

Lee et al. 2007 validated the use of peroxalate esters with fluorescent dyes for in vivo H_2O_2 imaging in the peritoneal cavity of mouse. The peroxalate nanoparticles had numerous attractive applications viz nanomolar sensitivity, tunable wavelength emission (460–630 nm), small size, specificity and deep-tissue-imaging capability [42]. An H_2O_2 sensor was developed based on the reaction of phenyl boronic acid with H_2O_2-ACPP (activatable cell-penetrating peptides) to detect H_2O_2 produced endogenously by macrophages, in a model of lung inflammation. The biosensor had an advantage of low micromolar sensitivity [43].

Nanoprobes

Jin H et al. 2010 optimized a new approach based on fluorescent SWCNT to understand the stochastic quenching events of H_2O_2 emission from epidermal growth factor (EGF)-stimulated human epidermal carcinoma cells. In response to EGF stimulation, local induction of 2 nM H_2O_2 in 50 min was done by this method [44]. Infrared fluorescent single-walled CNTs were used to investigate single-molecule efflux of H_2O_2 from human umbilical vein endothelial cells (HUVECs). As a result of angiogenic stimulation, a calibration curve of 12.5–400 nM H_2O_2 detection was obtained. The method has impressive sensitivity to nanomolar H_2O_2 detection with 300 nm spatial resolutions [45]. A new luminescent assay using iron oxide magnetic nanoparticles (MNPs) as peroxidase mimetics was designed by Wei and Wang [46]. The developed sensor exhibited strong sensitivity, as shown by its LOD as low as 3×10^{-6} mol/L with a linear range of 5×10^{-6} and 1×10^{-4} mol/L [46].

Emerging detection techniques for H_2O_2

A number of distinctive drawbacks exist in the above conventional H_2O_2 detection methods. Therefore, several efficient and convenient techniques were developed for the rapid detection of H_2O_2 in different samples. In the literature, various methods were reported for the electrochemical

estimation of H_2O_2. Table 2 summarizes the reported electrochemical methods revealing the electrode used, immobilization method, linearity, working pH and potential, sensitivity, LOD and their applications.

Biosensors

Biosensor is an analytical device that combines biological elements/molecules with microelectronic transducer devices to measure the concentration of analyte. It converts the biological response into electrical signals. An ideal biosensor must be highly specific, selective, accurate, reproducible and independent of interfering components. Biosensors can be classified into enzymatic and nonenzymatic biosensors according to the composition of the bio-recognition element [47]. H_2O_2 biosensors can be classified as follows (Fig. 2):

Potentiometric H_2O_2 biosensors

Potentiometric biosensors measure the electric potential of an electrode at zero current, which is actually the difference in potential between the working and standard electrode. These biosensors are based on the ion-selective electrodes to detect the target-specific ions during the biological reactions. In potentiometric biosensors, enzyme is immobilized onto the surface of electrode through glutaraldehyde crosslinking or adsorption process. The probe of pH meter is surrounded by the membrane, where biological reaction either produces or assimilates hydrogen ions. The variation in hydrogen ions causes a change in pH, which is measure of the concentration of analyte [48]. These potentiometric biosensors could be classified as follows depending on the type of electrode used:

Nafion membrane/Pt electrode

Parrilla et al. [49] used Nafion membrane/Pt electrode for potentiometric detection of H_2O_2. Nafion membrane has advantage of effective permselective barrier, which reduces the response to some redox-active species such as ascorbate. The coupling between redox potential on Pt electrode and Donnan potential plays a role in enhancement of sensitivity to H_2O_2. The current H_2O_2 biosensor showed sensitivity as 125.1 ± 5.9 mV/decade, linear range as 10–1000 µM and LOD as 10 µM [49].

MnO_2 doped/carbon paste electrode (CPE)

Manganese oxide (MnO_2)/carbon paste electrode was fabricated by Zheng [50]. The biosensor exhibited the sensitivity as 21–19.4 mV/decade, linear range as 0.3–363 µM and LOD as 0.12 µM. The analytical parameters of this biosensor were better than the latest potentiometric biosensor based on Nafion membrane/Pt electrode [49] except the sensitivity. It might be due to the use of MnO_2 and CPE-based electrode, as they both enhanced the surface area of the electrode and thus linear range and LOD. However, high sensitivity of Nafion membrane/Pt electrode was due to coupling between redox potential on Pt electrode and Donnan potential [50].

Amperometric H_2O_2 biosensor

Amperometric biosensors are based on generation of a current at a fixed potential applied between two electrodes. Like potentiometric biosensors, amperometric biosensors also exhibited analytical parameters such as response times, linear ranges, selectivity, reproducibility and sensitivities. The conventional amperometric biosensors were based on the Clark O_2 electrode. The electrode contained Pt cathode and Ag/AgCl standard electrode. The reduction of O_2 took place at Pt cathode vs Ag/AgCl as reference electrode. When a fixed potential relative to the reference electrode (Ag/AgCl) is tested on the working electrode (Pt cathode), it allows to generate current, which is directly proportional to the concentration of O_2. Normally both electrodes are kept into the concentrated KCl and kept them away from the bulk solution by employing O_2-permeable membrane onto them. The O_2 reduced at Pt cathode creates O_2 concentration effectively zero. Therefore, the degree of electrochemical reduction depends on the diffusion capacity of O_2 from the bulk solution [51].

Amperometric biosensors are further classified on the basis of generations used:

DO-metric first generation H_2O_2 biosensor

In dissolved oxygen (DO) metric biosensor, hemoglobin (Hb) protein has been immobilized onto the clark electrode surface for detection of H_2O_2. Hb molecule has four electroactive iron heme molecules, which enhance the electron transfer kinetics of heme proteins and help in biosensing application. The principle of biosensor is based on the two factors i.e., electrocatalytic activity of Hb and H_2O_2 reduction during measurement. In the present biosensor, Hb was immobilized onto Teflon membrane via glutaraldehyde crosslinking chemistry [52].

Second-generation H_2O_2 biosensor

An H_2O_2 biosensor, based on modified Au electrode, was fabricated by Kafi et al. 2007. They immobilized Hb onto Au electrode by electrochemical polymerization with o-PD. The fabricated biosensor exhibited good kinetic response, because of the direct immobilization of Hb. It also enhanced the sensitivity and selectivity of biosensor.

Table 2 Comparison of different analytic parameters of present H_2O_2 biosensor with those of earlier biosensors

S. no.	Support of immobilization	Method for immobilization	Type of biosensor	Linearity (μM)	Detection limit (LOD) μM	pH	Temp (°C)	Working potential. (V)	Sensitivity	Application	Ref.
1.	Nafion membrane/Pt electrode	Physical adsorption	Potentiometric	0.1–1000	0.1	NR	NR	NR	125.1 mV/decade	NR	[41]
2.	MnO_2 doped/CPE	Covalent binding	Potentiometric	0.3–363	0.12	NR	NR	NR	19.4 mV/decade	NR	[42]
3.	Hb/o-PD	Covalent binding	Amperometric	5–125	0.1	6.0	NR	NR	NR	NR	[45]
4.	HRP/AuNPs/CESM	Covalent binding	Amperometric	0.00001–2700	3	NR	NR	−0.1	NR	NR	[54]
5.	LSC/RGO/GCE	Covalent binding	Amperometric	1–16	0.7	NR	NR	NR	0.3 μAmp/mM/cm^2	NR	[58]
6.	ERGO/GCE	Covalent binding	Amperometric	1–16	0.7	7.0	NR	−0.25	300 μAmp/mM/cm^2	Real samples	[59]
7.	PB/Ru-HCF/GCE	Covalent binding	Amperometric	1.3–500	1.3	NR	NR	0	NR	NR	[60]
8.	CoPC-BOD	Covalent binding	Amperometric	0.001-10	0.001	NR	NR	−0.6	NR	NR	[61]
9.	Hb/NGP	Electrodeposition	Amperometric	10–150	8.24	7.0	25	0.20	NR	Blood	[62]
10.	Hb/Collagen microbelt	Electrospinning	Amperometric	5–30	0.37	7.0	20	−0.38	NR	Blood	[63]
11.	Hb/Ag sol films/GCE	Covalent binding	Amperometric	1–25	0.1	7.0	NR	−0.4	NR	Blood	[64]
12.	Hb/AuNPs/L-cys/p-ABSA/Pt disk	Electropolymerization	Amperometric	0.21–31	0.07	7.0	25	0.1	NR	Blood	[65]
13.	Hb/Collagen-mWCNT	Electrospinning	Amperometric	5–30	0.91	7.0	NR	−0.365	NR	Blood	[66]
14.	DNA-Hb/Au	Covalent binding	Amperometric	10–120	0.4	5.0	NR	−0.750	NR	Blood	[67]
15.	PtNPs/RGO/CS/Fc	Covalent binding	Amperometric	0.002–30	0.02	NR	37	−0.05	NR	Real samples	[68]
16.	DP-AuNP/HRP/GCE	Covalent binding	Amperometric	0.05–300	0.1	7.0	NR	−0.05	28.3 μAmp/mM/cm^2	Plasma	[69]
17.	GRCAPS/HRP/ITO	Covalent binding	Amperometric	0.01–12	3.3	7.0	37	−0.45	NR	Serum	[70]
18.	HRP/PAN-PNMThH	Covalent binding	Amperometric	0.005–60	3.2	6.0	NR	−0.25	35 μAmp/mM/cm^2	Sera and real samples	[71]
19.	TMB/HRP/PDMS/TEOS/SiO_2 NPs	Covalent binding	Colorimetric	4–72	1.3	5.0	NR	NR	NR	Real samples	[72]
20.	TTP/SPCE	Physical adsorption	Amperometric	20–500	4.1	7.0	NR	−0.1	NR	Blood	[73]
21.	GPtNPs	Covalent binding	Amperometric	0–0.32	0.001	NR	NR	0.45	811.26 μAmp/mM/cm^2	Blood	[74]
22.	PtRu/3DGF	Covalent binding	Amperometric	NR	0.04	7.4	NR	0.2	1023.1 μAmp/mM/cm^2	Biological	[75]
23.	Cytc/NiONPs/c-MWCNT/polyaniline/Au	Covalent binding	Amperometric	3–700	0.2	6.5	30	0.28	3.3 μAmp/mM/cm^2	Fruit juices	[76]
24.	HRP/toluidine/graphite powder/rigid ceramic	Covalent binding	Amperometric	0.429–455	0.171	7.0	NR	−0.25	NR	NR	[77]
25.	Hb/FFG/GCE	Covalent binding	Amperometric	0.5–500	0.1	7.0	NR	NR	NR	NR	[78]
26.	Catalase/Box/multicopper enzyme/GCE	Covalent binding	Amperometric	30–620	0.33	7.0	NR	0.2	21.34 μAmp/mM/cm^2	Blood and sera	[79]

Table 2 (continued)

S. no.	Support of immobilization	Method for immobilization	Type of biosensor	Linearity (μM)	Detection limit (LOD) μM	pH	Temp (°C)	Working potential. (V)	Sensitivity	Application	Ref.
27.	PtNF/N-graphene/ITO	Covalent binding	Amperometric	1–1000	340	7.2	NR	−0.4	61.23 μAmp/mM/cm^2	NR	[80]
28.	AuNPs/bipyridine nanobelts/GCE	Covalent binding	Amperometric	0.00009–0.0065	0.00045	7.0	NR	−0.1	283 μAmp/mM/cm^2	NR	[81]
29.	Microperoxidase-11 (MP-11)/metal-organic frameworks	Encapsulation	Amperometric	0.387–172.5	0.127	7.0	NR	0.2	168 μAmp/ mM/cm^2	NR	[82]
30.	pFeMOF/OMC	Encapsulation	Amperometric	0.5–70.5	0.45	NR	NR	NR	67.54 μA mM^{-1}	NR	[83]
31.	RGO/$CuFe_2O_4$/CPE	Covalent binding	Amperometric	2–200	0.52	NR	NR	NR	NR	NR	[84]
32.	HbNPs/Au	Covalent binding	Amperometric	1.0–1200	1	6.5	30	−0.2	129 ± 0.25 μA mM/ cm^2	Serum	[90]

Hb hemoglobin, *NGP-Pluronic P123* nanographene platelet, *L-cys* l-cysteine, *p-ABSA* paminobenzene sulfonic acid, *PtNPs* platinum nanoparticles, *RGO* reduced graphene oxide, *CS* chitosan, *FC* ferrocene carboxylic acid nano-hybrids, *DP* self-assembled dipeptide, *AuNP* gold nanoparticles, *HRP* horseradish peroxidase, *GCE* glassy carbon electrode, *GRCAPS* graphene capsules, *ITO* indium tin oxide, *PAN-PNMThH* poly (aniline-co-*N*-methylthionine), *ERGO* electrochemically reduced graphene oxide, *TMB* 3,3′,5,5′-teramethylbenzidine, *PDMS* polydimethylsiloxane, *TEOS* tetraethyl orthosilicate, SiO_2NPs silicon oxide nanoparticles, *TTP* turnip tissue paper, *Cyt c* cytochrome c, $NiONPs$ nickel oxide nanoparticles, *c-MWCNT* multiwall carbon nanotubes, *PANI* polyaniline, *HbNPs* hemoglobin nanoparticles, *Au* gold

The amperometric detection of H_2O_2 was carried out at − 300 mV in 0.1 M phosphate buffer solution (PBS) (pH 6.0). The biosensor showed a fast amperometric response towards H_2O_2. The levels of the relative standard deviation (RSDs) (< 3.5%) for the entire analysis reflected a highly reproducible sensor performance. Under the optimized conditions, LOD of the biosensor was 0.1 μM and linear range was from 5 to 125 μM. In addition, the sensor showed long-term stability and good sensitivity [53].

A sensitive amperometric HRP-based biosensor was fabricated via the deposition of AuNPs onto a three-dimensional (3D) porous carbonized chicken eggshell membrane (CESM). Due to the synergistic effects of the unique porous carbon architecture and well-distributed AuNPs, the enzyme-modified electrode showed an excellent electrochemical redox behavior. Compared with bare GC electrode, the cathodic peak current of the enzyme electrode was increased 12.6 times at a formal potential of − 100 mV (vs. SCE) but charge-transfer resistance decreased to 62.8%. Additionally, the AuNPs-CESM electrode exhibited a good biocompatibility, which effectively retains its bioactivity with a surface coverage of HRP 6.39×10^{-9} mol cm^{-2} (752 times higher than the theoretical monolayer coverage of HRP). Furthermore, the HRP-AuNPs-CESM-GC electrode, s had a good accuracy and high sensitivity with the linear range of 10–2700 μM H_2O_2 and the LOD of 3 μM H_2O_2 ($S/N = 3$) [54].

A simple and low-cost H_2O_2 biosensor was developed using a *Yucca filamentosa* plant leaf membrane in conjunction with an O_2 sensor. The leaf membrane contained H_2O_2 peroxidase, which decomposed H_2O_2 to produce O_2. The response rate was faster for a *Yucca* membrane (t_{90} response time is ≈ 14 s) than a *Yucca* membrane with the O_2-permeable membrane (t_{90} response time is ≈ 200 s) and the sensitivity was much improved. The biosensor exhibited an excellent linear calibration range from 85 μM to 3750 μM M, H_2O_2 (correlation coefficient $r = 0.9999$) with a LOD of 15.1 μM and repeatability (1.024%, $n = 10$). The effects of pH and temperature on the response of the H_2O_2 biosensor were studied in detail. The working life-time of the biosensor was good, as it retained 86.7% of its initial sensitivity at 25 °C even after 2350 determinations of H_2O_2 sample solutions. It was successfully applied for determination of H_2O_2 concentration in some commercial samples [55].

A simple and low-cost H_2O_2 biosensor was fabricated using a beef liver catalase-immobilized eggshell membrane and a dissolved O_2 electrode. Catalase from beef liver extract was covalently immobilized on an eggshell membrane and subsequently covered the surface of an O_2 electrode. The detection scheme was based on the increase in dissolved O_2 content upon exposure to H_2O_2 solution. The increase in O_2 level was then monitored and related to the H_2O_2 concentration. The effects of enzyme loading, dissolved O_2 content,

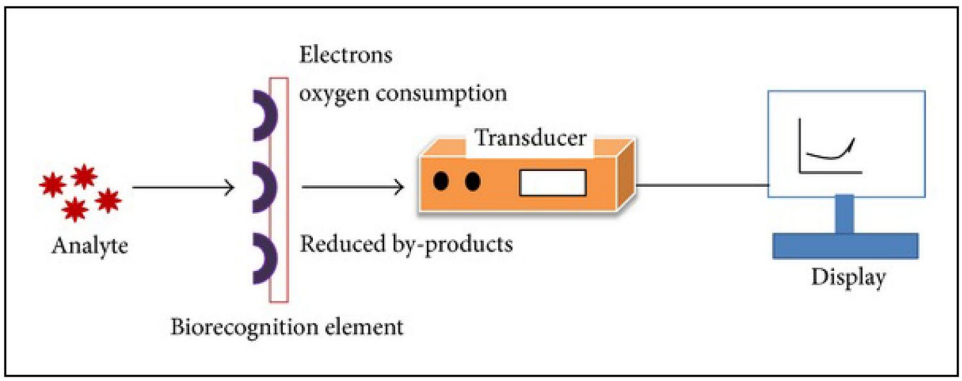

Fig. 2 Basic principle of biosensor

pH, phosphate buffer concentration and temperature on the biosensor were also studied. The response and recovery times of the biosensor (t95) were 1 min, respectively. The detection limit based on 3σb was 3 µM and the relative standard deviation of the response was 1.28% ($n = 10$) for a solution containing 300 µM of H_2O_2. The H_2O_2 biosensor demonstrated a reasonable long and stable shelf-life. It was successfully applied to the determination of H_2O_2 concentration in some commercial samples [56].

Overall, second generation biosensors exhibited linear range between 5 and 3750 µM and LOD between 0.1 and 15.1 µM. Kaafi et al. 2007 exhibited better LOD as compared to other biosensors due to direct immobilization of Hb onto Au electrode, which enhanced the electrochemical performance of biosensor. However, Yucca membrane-based H_2O_2 biosensor showed wider linear range, due to high catalytical efficiency of Yucca membrane.

Third-generation H_2O_2 biosensor

Nanomaterial electrode-based biosensors are further classified as membrane-based and electrode-based biosensors.

Electrode composition based biosensor Electrode-based biosensors can be classified on the basis of nanocomposites used in their synthesis:

MWCNTs-nanoNiO/glassy carbon (GCE) A biosensor based on catalase/MWCNTs-nanoNiO composite/GC electrode was employed for detection of H_2O_2. The immobilized catalase displayed excellent electrocatalytic activity towards the reduction of H_2O_2. The developed amperometric biosensor expressed a wider linear range, 200–2.53 mM and LOD of 19.0 µM. The electrochemical impedance measurements revealed that the charge transfer resistance was dropped significantly after enzymatic reaction of nanobiosensor with H_2O_2. The biosensor was highly sensitive to H_2O_2 over a linear range of 19–170 nM with a LOD of 2.4 nM [57].

$La_{0.6}Sr_{0.4}CoO_{3-\delta}$ (LSC) perovskite oxide/-reduced graphene oxide (RGO) GC electrode $La_{0.6}Sr_{0.4}CoO_{3-\delta}$ (LSC) perovskite oxide/-reduced graphene oxide(RGO)-based enzymeless biosensor was designed for detection of H_2O_2. This biosensor overcame the problems of enzyme-based biosensor, as LSC was not sensitive to the pH, temperature, humidity and poisoning chemicals. Moreover, LSC offered high electroactive properties towards the catalytic function of H_2O_2. Additionally, RGO could be added to optimize the analytical performance of biosensor. The working electrode LSC /RGO/GCE exhibited high sensitivity of 500 µA mM^{-1} cm^{-2} for H_2O_2 and LOD of 0.05 µM, respectively (at $S/N = 3$). The biosensor showed linearity in the concentration range from 0.2 to 3350 µM [58].

Electronic-reduced graphene oxide (ERGO)/GCE A simple, facile and reproducible non-enzymatic H_2O_2 sensor was developed using electrochemically reduced graphene oxide (ERGO)-modified GC electrode. The modified GC electrode was characterized by FTIR, UV–Visible spectra, SEM and atomic force microscopy (AFM). Cyclic voltammetric (CV) analysis revealed that ERGO/GCE exhibited virtuous charge transfer properties for a standard redox systems and showed excellent performance towards electro-reduction of H_2O_2. Amperometric study using ERGO/GCE exhibited high sensitivity (0.3 µA/µM) and faster response upon the addition of H_2O_2 at an applied potential of −0.25 V vs Ag/AgCl. The LOD was 0.7 µM ($S/N = 3$) and the time to reach a stable steady state current was < 3 s for a linear range of H_2O_2 concentration (1–16 µM). In addition, the modified GC electrode had good reproducibility and long-term stability [59].

Prussian blue (PB)/ruthenium oxide hexacyanoferrate/GCE A sensor for amperometric detection of H_2O_2 based on Prussian blue (PB)/ruthenium oxide hexacyanoferrate/GC electrode was developed. The electrocatalytic process allowed the determination of H_2O_2 at 0.0 V with a LOD of 1.3 µmol L^{-1} in a flow-injection analysis (FIA) configuration. Under optimal FIA operational conditions, the linear response of the method was extended up to 500 µmol L^{-1} H_2O_2 with good stability. The possibility of using the developed sensor in medium-containing sodium ions and the increased operational stability constitute advantages in comparison with PB-based amperometric sensors. The usefulness of the methodology was demonstrated by

addition-recovery experiments with rainwater samples and values were in the 98.8–103% range [60].

Cobalt phthalocyanine-modified boron-doped diamond electrode A cobalt phthalocyanine-modified boron-doped diamond (CoPc-BDD) electrode was fabricated. The hydrogen-terminated BDD electrode surface was terminated with the pyridine moieties via photochemical modification with 4-vinylpyridine (4VP), followed by immobilization of CoPc on the surface by immersion of the 4VP-BDD samples in a CoPc solution. X-ray photoelectron spectroscopy studies suggested that coordination of the surface pyridine to the Co atom in CoPc contributes to the surface modification. Electrochemical detection of hydrogen peroxide at the modified electrode was also investigated. Cyclic voltammetry confirmed that the CoPc-BDD electrode exhibits catalytic activity for the electrochemical oxidation of H2O2. Using a flow-injection analysis-electrochemical detection (FIA-EC) system, CoPc-BDD electrode was showed following analytic parameters: Linear range: 10 nM–10 µM, LOD: 10 nM, working potential: − 0.6V [61].

Hb [pluronic P123-nanographene platelet(NGP)] electrode An amperometric H_2O_2 biosensor was fabricated by immobilizing Hb on a pluronic P123-nanographene platelet (NGP) composite. The surface concentration (Γ^*) and apparent heterogeneous electron transfer rate constant (k_s) were $1.60 \pm 0.17 \times 10^{-10}$ mol cm^{-2} and 48.51 s^{-1}, respectively. In addition, the Hb/Pluronic P123-NGP composite showed excellent bio-electrocatalytic activity toward the reduction of H_2O_2. The biosensor exhibited a linear response to H_2O_2 in the range of 10–150 µM and a LOD of 8.24 µM ($S/N = 3$) at 0.20 V, pH-7.0 and 25 °C. The apparent Michaelis–Menten constant (K_{mapp}) was 45.35 µM .The resulting biosensor showed fast amperometric response, with very high sensitivity, reliability and effectiveness [62].

Electrospun Hb–collagen composite A hemoglobin (Hb)–collagen microbelt-modified electrode with three-dimensional configuration was fabricated via the electrospinning method. Direct electron transfer of the Hb immobilized into the electrospun collagen microbelts was greatly facilitated. The apparent heterogeneous electron transfer rate constant (k_s) was calculated to be 270.6 s^{-1}. The electrospun Hb–collagen microbelt-modified electrode showed an excellent bioelectrocatalytic activity toward the reduction of H_2O_2 at pH 7.0 and 20 °C. The amperometric response of the biosensor varied linearly with the H_2O_2 concentration ranging from 5×10^{-6} mol L^{-1} to 30×10^{-6} mol L^{-1}, with a LOD of 0.37×10^{-6} mol L^{-1} (signal-to-noise ratio of 3). The K_{mapp} was 77.7 µmol L^{-1}. The biosensor exhibited fast amperometric response, high sensitivity, good reproducibility and stability [63].

Hb/Ag sol films/GCE A novel amperometric electrochemical H_2O_2 biosensor was fabricated by immobilizing hemoglobin–silver (Hb–Ag) sol onto GC electrode, which showed a sensitive response to the reduction of H_2O_2 without any electron mediator. Ultraviolet–visible (UV–vis) spectra and reflectance absorption infrared (RAIR) spectra of Hb-Ag/GC suggested that Hb in Hb–Ag sol retained its native secondary structure. Scanning electron microscopy (SEM) demonstrated that the morphology of the Hb film was much different from the Hb–Ag sol film. The Hb–Ag film exhibited a good electrocatalytic activity for the reduction of H_2O_2. Under optimum conditions (at − 0.4V and pH 7.0), the biosensor exhibited linearity for H_2O_2 in the concentration range 1–25 µM and LOD as 0.1 µM at 3σ. The biosensor exhibited high sensibility, good reproducibility, and long-term stability [64].

Gold nanoparticles (AuNPs)/cysteine (L-Cys)/poly(p-aminobenzene sulfonic acid) (ABSA)-based platinum disk electrode An H_2O_2 biosensor was fabricated by self-assembling Hb, nano-Au and L-cysteine (L-cys) on the precursor film formed by electropolymerization of p-aminobenzene sulfonic acid (p-ABSA) on the Pt disk electrode. The EIS and UV–Vis absorption spectroscopy of Hb/AuNPs/L-cys/p-ABSA were carried out to characterize the fabrication process. The biosensor response and factors influencing the biosensor were studied by CV and chronoamperometry. The immobilized Hb showed direct electrochemical behavior toward the reduction of H_2O_2. The biosensor exhibited linear range as 0.21–31 µM and LOD as 0.07 µM ($S/N = 3$) at 0.1 V, pH: 7.0 and 25 °C. In addition, the biosensor exhibited good accuracy and high sensitivity [65].

Hb–collagen-CNTs An Hb–collagen-CNTs nanofibers modified electrode was constructed by incorporating CNTs into the composite of Hb and collagen, using co-electrospinning technology. The formed Hb–collagen-CNTs composite nanofibers possessed distinct advantage of three-dimensional porous structure, biocompatibility and excellent stability. Hb immobilized in the electrospun nanofibers retained its natural structure .The heterogeneous electron transfer rate constant (k_s) of the direct electron transfer between Hb and electrodes was 5.3 s^{-1}. In addition, the electrospun Hb–collagen-CNT nanofiber-modified electrodes showed good electrocatalytic properties toward H_2O_2 with a linear concentration range, 5–30 µM and LOD of 0.91 µM ($S/N = 3$) and K_{mapp} of 32.6 µM at − 0.365 V and pH 7.0 [66].

DNA/Hb/Au A H_2O_2 biosensor was designed by dropletting of DNA and Hb onto Au electrode surface layer by layer. The sensor based on the direct electron transfer of iron of Hb showed a well electrocatalytic response to the reduction of the H_2O_2. This sensor offered an excellent electrochemical response for H_2O_2 concentration below micromole level with high sensitivity and selectivity and short response time. The levels of the RSD's (< 5%) for the entire analyses reflected the high reproducibility of the sensor. Using the optimized conditions (potential − 0.75 and pH 5.0), the

linearity for H_2O_2 detection was 10–120 µM with LOD of 0.4 µM ($S/N = 3$) [67].

Platinum nanoparticles (PtNPs)/reduced graphene oxide (RGO)–chitosan (CS)–ferrocene (Fc) carboxylic acid nano-hybrids (Pt NPs/RGO-CS-Fc) A highly sensitive non-enzymatic electrochemical sensor based on platinum nanoparticles/reduced graphene oxide–chitosan–ferrocene carboxylic acid nano-hybrids (Pt NPs/RGO-CS-Fc biosensor) was developed for the measurement of H_2O_2. The RGO-CS-Fc nano-hybrids were characterized by UV–Vis spectrum, FTIR spectroscopy, TEM, Raman spectrometry and EIS. Under optimal experimental conditions, the Pt NPs/RGO-CS-Fc biosensor showed outstanding catalytic activity toward H_2O_2 reduction. The biosensor showed current response at − 0.05 V and 37 °C, a linear relationship with H_2O_2 concentration from 2.0×10^{-8} to 3.0×10^{-6} M with a correlation coefficient (R^2) of 0.9968 and with log H_2O_2 conc. from 6.0×10^{-6}M to 1.0×10^{-2} M with a correlation coefficient (R^2) of 0.9887, the LOD of 20 nM was obtained at the signal/noise (S/N) ratio of 3. Moreover, the Pt NPs/RGO-CS-Fc biosensor exhibited excellent anti-interference capability and reproducibility for the detection of H_2O_2. The biosensor was successfully applied for detection of H_2O_2 from living cells containing normal and cancer cells. All these results proved that the Pt NPs/RGO-CS-Fc biosensor had the potential application in clinical diagnostics to evaluate oxidative stress of different living cells [68].

Dipeptide–AuNP/HRP/GCE A mediate H_2O_2 biosensor was developed based on HRP/dipeptide–AuNP hybrid spheres modified GC electrode. The self-assembled diphenylalanine (FF) or dipeptide(DP)–AuNPs hybrid microspheres with a hollow structure were prepared in aqueous solution by a simple one-step method. The TEM and SEM images of DP-AuNPs hybrid and working electrode showed that formed AuNPs were localized both inside and on the surface of DP spheres. HRP as a model enzyme was further immobilized onto DP–AuNPs hybrid spheres to construct a mediate H_2O_2 amperometric biosensor. UV–Vis spectroscopic study revealed that the immobilized HRP retained its original structure. CV study of HRP/dipeptide–AuNP hybrid spheres/GC electrode showed high electrocatalytic activity to H_2O_2. The biosensor exhibited a wide linear range of 0.05–300 µM with a high sensitivity of 28.3 µA mM^{-1} and LOD of 0.1 µM ($S/N = 3$) at 0.05 V and pH 7.0. The biosensor exhibited good reproducibility and long-term stability. Thus, dipeptide-AuNP hybrid sphere was proved to be a promising matrix for application in the fabrication of electrochemical biosensors, due to its excellent biocompatibility and good charge-transfer ability [69].

Graphene capsules (GRCAPS)/horseradish peroxidase (HRP)/indium titanium oxide (ITO) To solve the problems of enzymatic loss and inactivation of the biosensor, HRP was initially encapsulated in graphene capsules (GRCAPS) using porous $CaCO_3$ as sacrificial templates to mimic the existence form of bio-enzymes in the organisms, and then GRCAPS and graphene-poly (sodium 4-styrenesulfonate) were assembled onto the substrate of indium tin oxide (ITO) for constructing multilayer films of the biosensor. TEM and field-emission SEM analyses revealed that GRCAPS and multilayer films were prepared. The resulting biosensor showed a wide linear range of 0.01–12 µM and, LOD of 3.3 µM ($S/N = 3$), excellent anti-interference ability, and long-term stability under optimum condition at − 0.45V, pH 7.0 and 37 °C [70].

HRP/poly (aniline-co-N-*methylthionine) (PAN-PNMThH)* A H_2O_2 biosensor was fabricated using electrochemical doping to immobilize HRP in a new conducting polymer, poly(aniline-co-N-methylthionine) (PAN-PNMThH). Amperometric detection of H_2O_2 was evaluated by holding the PAN-PNMThH HRP electrode at − 0.25 V [versus saturated calomel electrode (SCE)]. PAN-PNMThH showed excellent redox activity and high porosity and acted as an electron transfer mediator. The biosensor showed a wide linear range from 5.0 µM to 60.0 mM H_2O_2 with a sensitivity of 35 mA M^{-1} cm^{-2}, a LOD of 3.2 µM (S/N ratio of 3) and a K_{mapp} of 2.79 mM at pH 6.0. The biosensor had good analytical performance and storage stability [71].

3,3′,5,5′-teramethyl bencidine (TMB)/polydimethylsiloxane (PDMS)/tetraethyl orthosilicate (TEOS)/silicon oxide nanoparticles (SiO_2NPs) A H_2O_2 biosensor was fabricated based on the co-immobilization of the reagent 3,3′,5,5′-teramethylbenzidine (TMB) and HRP in a PDMS-TEOS-SiO_2NPs support to enhance the performance of colorimetric biosensors. The HRP, in presence of H_2O_2, catalyzes the oxidation of TMB, producing a blue color. The generated biosensor, doped with the substrate (TMB) and HRP (entrapped or adsorbed), was used to determine H_2O_2 in real samples. Firstly, the immobilization of TMB and HRP in the composite was studied to find the best suitable configuration. The kinetic parameters i.e., V_{max} and K_{mapp} of the different assayed systems were n determined and compared. Second, the analytical properties of the H_2O_2 method were studied. The biosensor was simple, inexpensive, highly sensitive and selective for determination of H_2O_2, with LOD of 1.3 µM and a good linearity in the range 4.2–72 µM at pH 7.0. The LOD could be improved to 0.4 µM by acidifying the solution with sulphuric acid. The relative standard deviation (RSD) was < 10%. The biosensor had a reagent-release support, which significantly simplified the analytical measurements, as it avoided the need to prepare derivatization reagents and sample handling. It allowed in situ measurements [72].

Turnip tissue paper (TTP)/screen-printed carbon electrode (SPCE) A novel inexpensive turnip tissue paper-based mediated amperometric H_2O_2 biosensor was developed based on screen-printed carbon electrodes (SPCEs). The use of cellulose paper proved to be an "ideal" and simple

biocompatible immobilization matrix for raw turnip peroxidase as it was successfully embedded within the fiber matrix of paper via physical adsorption. The mediator potassium hexacyanoferrate (II) was also embedded onto the paper matrix together with the raw enzyme. The biosensor allowed a minute amount (0.5 µL) of sample solution for analysis. The biosensor had a linear range as 20–500 µM, LOD as 4.1 µM, at − 0.1 V, pH, 7.0, correlation coefficient (R^2) as 0.999, retention capacity as 70% of initial activity and storage stability—25 days at 4 °C. The biosensor was employed for analysis and the results matched with the classical titration method [73].

Graphene-supported platinum nanostructure (GPtNPs) A facile and highly sensitive platform was developed for synthesizing branched Pt nanostructures on graphene. Graphene support was employed to increase the performance of platinum nanostructures (PtNs) in electrochemical sensing/biosensing. The graphene-supported PtNs (GPtNs)-modified electrode efficiently oxidises the H_2O_2 at a lower potential in neutral phosphate buffer without employing the enzymes or redox mediators. The GPtNs electrode exhibited high sensitivity of 811.26 µAmM^{-1} cm and linear range, 0–0.32 mM, with a very low LOD (1 nM) for H_2O_2 at potential 0.45 V and pH 7.0. The sensor showed excellent reproducibility, long-time storage and operational stability. It measured H_2O_2 concentration in the real samples (rainwater) [74].

Platinium–ruthenium (PtRu)/three-dimensional graphene flakes (3DGF) An amperometric H_2O_2 biosensor was developed exploiting the large surface, excellent dispersion and high degree of sensitivity of bimetallic nanocatalysts. To achieve it, graphene foam (GF), a three-dimensional (3D) porous architecture consisting of extremely large surface and high-conductive pathways was incorporated into platinum–ruthenium (PtRu) bimetallic nanoparticles, as an electrochemical nanocatalyst for detection of H_2O_2. PtRu/3D GF nanocatalyst brought electrochemical oxidation of H_2O_2 without any additional mediator showing a high sensitivity (1023.1 µA $mM^{-1}cm^{-2}$) and a LOD of 0.04 µM for H_2O_2 at 0.2 V and pH 7.4. The amperometric results revealed that GF provided a promising platform for the development of electrochemical sensors in biosensing and PtRu/3D GF nanocatalyst possessed the excellent catalytic activity toward the H_2O_2 detection. A small particle size and a high degree of the dispersion in obtaining of large active surface area were important for the nanocatalyst for the best H_2O_2 detection in biosensing. Ascorbic acid and uric acid had practically no effect [75].

Cytochrome C (Cytc)/nickel oxide nanoparticles (NiONPs)/multiwalled carboxylated carbon nanotubes (c-MWCNT)/polyaniline/Au An amperometric H_2O_2 biosensor was constructed based on covalent immobilization of Cytochrome c onto nickel oxide nanoparticles/carboxylated multiwalled carbon nanotubes/polyaniline composite (NiO-NPs/cMWCNT/PANI) electrodeposited onto Au electrode. The modified Au electrode was characterized by CV, EIS, SEM and FTIR spectroscopy. CV studies of the electrode at different stages demonstrated that the modified Au electrode had enhanced electrochemical oxidation of H_2O_2, which offered a number of attractive features to develop an amperometric biosensor based on split of H_2O_2. There was a good linear relationship between the current (mA) and H_2O_2 concentration in the range 3–700 µM at − 0.28 V, pH 6.5 and 30 °C. The sensor had a LOD of 0.2 µM ($S/N = 3$) with a high sensitivity of 3.3 mA μM^{-1} cm^{-2} .It measured accurately the level of H_2O_2 in different fruit juices [76].

HRP/toluidine/graphite powder/rigid ceramic HRP and water-soluble mediator toluidine blue were immobilized covalently onto 3-aminopropyl trimethoxy silane precursor through glutaraldehyde crosslinker. A rigid ceramic composite electrode was constructed from this modified silane along with graphite powder, which caused electrochemical oxidation of H_2O_2, as proved by CV studies in the potential range, 0.2V to -0.4V vs SCE. The biosensor showed a stable voltammogram with cathodic peak at − 0.234 V and anodic peak at − 0.172 V, with a formal potential of − 0.203 V. The biosensor was optimized. The biosensor exhibited linearity in the range, 0.429 µM–0.455 mM with a LOD of 0.171 µM at − 0.25 V, pH 7.0 and 30 °C. The biosensor was robust for long-term usage besides showing the high sensitivity, rapid response and an advantage of surface renewability by simple mechanical polishing [77].

Hb/dipeptide graphene nanostructure/GCE Hb was immobilized onto self-assembled nanowires of diphenylalanine (FF) and graphene (G) nanocomposite-modified GC electrode to fabricate an amperometric H_2O_2 biosensor. The immobilized Hb, retained its original structure and bioactivity, as revealed by UV spectroscopy. The Hb/FF-G/GC electrode exhibited high electrocatalytic activity to H_2O_2, with wider linearity in the range, 5.0×10^{-7} to 5.0×10^{-4} mol L^{-1}, with a LODf 1.0×10^{-7} mol L^{-1} at pH 7.0. These results indicated the excellent biocompatibility and good charge-transfer ability of nanowires of FF-G nanocomposites [78].

Catalase/bilirubin oxidase/multi-copper enzyme/carbon nanotube-modified electrodes (catalase/box/multicopper enzyme/GCE) A highly sensitive and selective amperometric H_2O_2 biosensor was developed based on adsorption of catalase (Cat) and either laccase (Lac) or bilirubin oxidase (BOX) onto MWCNT-modified GC electrode. The stability and durability of the electrode was improved by glutaraldehyde crosslinking of enzymes. CV and chrono-amperometry proved the synergy of the laccase and catalase co-adsorbed on MWCNT. Catalase catalyzed the transformation of H_2O_2 into H_2O and O_2, which was further changed into water by multi-copper enzymes (MCO), either laccase or bilirubin oxidase. The unique property of such a bienzymatic sensing layer was able to detect O_2 originating both from catalase

activity and the self-decomposition of H_2O_2. This helped in evaluating the initial concentration of H_2O_2 in the analyzed sample [79].

Platinum nanoflower and graphene modified indium titanium electrode (PtNF/N-graphene/ITO) The nitrogen-doped graphene (*N*-graphene) was synthesized by annealing graphene oxide with urea at 900 °C. A non-enzymatic H_2O_2 biosensor was fabricated by a simple layer-by-layer electrophoretic and electrochemical sequential deposition of nitrogen-doped graphene (*N*-graphene) and Pt nanoflower (Pt NF) with different *N*-graphene loadings, onto ITO-coated glass plate. The structure and morphology of PtNF/*N*-graphene/ITO electrode were studied by XRD field emission electron microscopy (FEEM), TEM, Raman and X-ray photoelectron spectra. The Pt NF-*N*-graphene-modified ITO electrodes with different *N*-graphene loadings were used as a non-enzymatic electrode for detection of H_2O_2. The Pt NF-*N*-graphene-modified ITO electrode with a 0.05 mg ml^{-1} *N*-graphene loading showed the linearity in the range, 1–1000 µM with LOD as 340 µM at pH 7.2 and − 0.4 V. It also exhibited excellent stability and reproducibility for non-enzymatic H_2O_2 detection because of the synergistic effect between the electrocatalytic activity of Pt NF and the high conductivity and large surface area of *N*-graphene [80].

Gold nanoparticle-decorated silver-bipyridine nanobelts (AuNPs/bipyridine nanobelts/GCE) AuNPs modified with 4-mercaptopyridine and 6-mercapto-1-hexanol were employed as coordination agents to prepare a novel hybrid nanomaterial with Ag:4,4′-bipyridine nanobelts. This nanohybrid was electrodeposited onto GC electrodes. A mediatorless amperometric biosensor for H_2O_2 was constructed by immobilizing HRP onto this modified GC electrode. The electrode showed a rapid response within 4 s at − 0.1 V and pH 7.0 and a linearity in the range, 90 pM–6.5 nM with a LOD of 45 nM ($S/N = 3.0$) for H_2O_2. The biosensor had a high sensitivity of 283 A/M cm^2. The enzyme electrode retained 96 and 78% of its initial activity after 15 and 30 days of storage at 4 °C, respectively [81].

Metal-organic framework-based electrode A new Co-metal-organic framework [Co(pbda)(4,4-bpy)·$2H_2O$]n Co-MOF] [bpy = 4,4-Bipyridine; H_2pbda = 3-(pyridine-3-yloxy) benzene-1,2-dicarboxylic acid] or CoMOF was synthesized under hydrothermal conditions and then electrodeposited onto GC electrode to construct a high performance amperometric H_2O_2 sensor. Single-crystal X-ray analysis exhibited a three-dimensional supramolecular architecture with a uninodal 4-connected net with the gis topology. The CV of the Co-MOF-modified GC electrode showed a pair of reduction peaks at ca. − 0.40 V in 0.1 M NaOH solution corresponding to CoIII-MOF/CoII-MOF couple. The highly electrocatalytic activity of the Co-MOF-modified GC electrode on H_2O_2 reduction showed a wide linear range from 5 µM to 9.0 mM, a low detection limit of 3.76 µM and a high sensitivity of 83.10 µA/mM cm^2 at an applied potential of − 0.40 V. Further, the sensor had favorable selectivity and long-term stability. The Co-MOF possessed highly efficient intrinsic peroxidase-like activity to produce hydroxyl radical from H_2O_2, which react with oxidized peroxidase substrate (terephthalic acid) to produce color [82].

Porphyrinic iron-based metal-organic framework/ordered mesoporous carbon (pFeMOF/OMC) A novel hybrid of porphyrinic iron metal-organic framework (pFeMOF) and ordered mesoporous carbon (OMC) was synthesized via a simple one-step hydrothermal method. This hybrid was electrodeposited onto GC electrode for non-enzymic amperometric determination of H_2O_2, released from viable cells. The pFeMOF/OMC hybrid materials were synthesized Fe (III) ion could coordinate with carboxylates of porphyrin groups strongly, leading to more stable MOFs. As pFeMOF mimic peroxidase property, the electrode gave amplified electrochemical signal. The carbon skeleton of OMC revealed a function of restriction for the growth of pFeMOF crystallites, resulting in more active sites to reduce H_2O_2. The increased amount of mesoporous brings faster diffusion. Moreover, the electrical conductivity and stability was improved due to the introduction of OMC. The electrocatalytic reduction of H_2O_2 displayed two segments linearity range from 0.5 to 70.5 µM and 70.5 to 1830.5 µM, with high sensitivity of 67.54 µAmM^{-1} in low concentration range and 22.29 µAmM^{-1} of high concentration. The LOD was as low as 0.45 µM. The pFeMOF/OMC/GC electrode showed outstanding property to resist interference, long-term stability and repeatability. Due to these excellent analytical performances, the sensor was able to detect H_2O_2 satisfactorily released from living cells [83].

Carbon paste electrode modified with nano-composite of reduced graphene oxide and $CuFe_2O_4$ nanoparticles A highly sensitive voltammetric H_2O_2 sensor (RGO/$CuFe_2O_4$/CPE) was developed by modifying a carbon paste electrode(CPE) with reduced graphene oxide (RGO) and $CuFe_2O_4$ nanoparticle $CuFe_2O_4$ nanoparticles were synthesized by co-precipitation method and characterized by SEM, TEM, XRD, and FTIR. The electrocatalytic reduction of H_2O_2 was measured by CV chronoamperometry, amperometry and differential pulse voltammetry (DPV). Under the optimum conditions (pH 5.0), the modified CP electrode showed a fast amperometric response within < 2 s, a good linear range of 2–200 µM, LOD of 0.52 µM for H_2O_2. The current obtained through DPV, was increased linearly with increase in H_2O_2 concentration in the ranges, 2–10 µM and 10–1000 µM with LOD as 0.064 µM The sensor measured H_2O_2 level in biological and pharmaceutical samples such as milk, green tea, and hair dye cream and mouthwash solution [84].

Carbon-supported Cu@Pt core-shell nanoparticles A nanocomposite of carbon-supported Cu@Pt/C core-shell

nanoparticles was synthesized via two-step reduction method. The electrochemical sensor based on Cu@Pt/C showed better electrocatalytic activity for the reduction of H_2O_2 than that based on Pt/C. The Cu@Pt/C sensor had a wide linear range between 0.50 µM and 32.56 mM, with a high sensitivity of 351.3 µA mM^{-1} cm^{-2}, and LOD of 0.15 µM ($S/N = 3$). The sensor exhibited excellent long-time stability, good reproducibility and acceptable selectivity [85].

Ratiometric fluorescent-based H_2O_2 biosensor

The ratiometric fluorescent biosensing of H_2O_2 is based on the facility of dLys-AgNCs ratiometric probe, assigned to the ability of lysozyme (dLys) to work as a stabilizing agent as well as fluorescence signal unit. In the presence of Fenton reagents, dLys-AgNCs emission at 640 nm was quenched by·OH, whereas the emission at 450 was improved as a result of·OH-induced oxidation of tyrosine in the lysozyme. This probe was applied for extreme sensitive determination of H_2O_2. The fluorescence changes of F450/F640 had wider linearity for H_2O_2 in the range, 0.8–200 µmol/L ($R^2 = 0.9993$), with a LOD as 0.2 µmol/L. The dLys-AgNCs also had a sensitive response to variation of ·OH levels in living cells, which showed its promising application for studying ·OH-induced oxidative damage to proteins [86] (Fig. 3).

Chemiluminescence-based H_2O_2 biosensor

The chemiluminescence-based H_2O_2 biosensor was fabricated using poly(ethylene-co-polyvinyl alcohol) (PVA-co-PE) membrane. The PVA-co-PE nanofibers (Av. diameter in the range from 200 to 500 nm) were modified by cyanuric chloride and 1,3-propanediamine and subsequently biotinylated, then HRP was immobilized onto this membrane. The HRP-immobilized PVA-co-PE nanofiber membrane showed high activity, efficiency, sensitivity and reusability, when used for the luminol-H_2O_2 reaction. The relative light unit (RLU) could run up to 5×10^{11} µM, when the concentration of H_2O_2 was as low to 10^{-9} µM. In the biosensor, the HRP-immobilized onto the PVA-co-PE nanofiber membrane, which acted as potential chemiluminescence transducer [87].

Supercapacitor-based H_2O_2 biosensor

Tellurium nanoparticles (Te Nps)-based H_2O_2 biosensor exhibited specific capacitance (586 F/g) at 2 mA/cm^2 and 100 F/g at 30 mA/cm^2 with an excellent cycle life (100% after 1000 cycles). The biosensor exhibited better analytical performances such as, linear range of 0.67–8.04 µM for H_2O_2, high sensitivity (0.83 mA mM^{-1} cm^{-2}) with good correlation coefficient i.e., 0.995. The response time was < 5 s [88].

Nanoneedle-based H_2O_2 biosensor

A biosensor based on $KNbO_3$ nanoneedles (KNs) was constructed to catalyze H_2O_2, directly. The mechanism of detection was based on molecular orbital principles, with the development of σ-bonding within e_g orbital of surface niobium ions and surface-adsorbed oxygen-related intermediate species. It allows the direct electron transfer between HRP and electrode surface. The designed biosensor revealed high sensitivity of 750 µA mM^{-1} cm^{-2} and rapid response i.e. 1–2 s towards H_2O_2 [89].

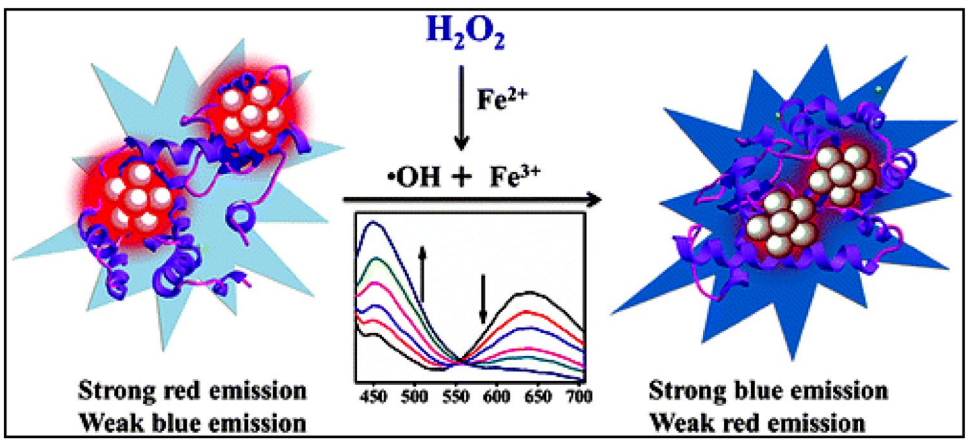

Fig. 3 Schematic representation of ratiometric fluorescent biosensing of hydrogen peroxide

Protein nanoparticle-based H_2O_2 biosensor

A new approach of construction of a nanomaterial based-but simple amperometric H_2O_2 biosensor was designed by Narwal et al. 2017. The biosensor was developed by covalent immobilization of haemoglobin nanoparticles (HbNPs) onto polycrystalline Au electrode. The working electrode exhibited optimum response at pH 6.5 and 30 °C. A linear range of 1–1200 µM with a LOD of 1.0 µM, 2 V against Ag/AgCl with rapid response time of 2.5 s. The HbNPs/AuE offered Vmax of 5.161 ± 0.1 µA cm^{-2} with Michaelis–Menten constant Km of 0.1 ± 0.01 mM and sensitivity of 129 ± 0.25 µA cm^{-2} mM^{-1}. The measured analytical recovery of biosensor was 98.01%. Within and between batch coefficients of variation (CV) were 3.16 and 3.36%, respectively. The biosensor showed a good correlation coefficient ($r = 0.99$) between standard method and present method. The HbNPs/Au electrode lost 10% of its initial activity after 90 days of its regular uses, when stored dry at 4 °C. The biosensor-measured H_2O_2 in blood of diabetic patients [90].

A comparison of various electrochemical H_2O_2 biosensors is summarized in the Table 2.

Technical challenges in detection of hydrogen peroxide

Lack of reliability, false-positive results, cost, portability, lower detection limit, interferences, and careful calibration are potential methodological challenges of non-electrochemical methods. This would likely to limit the use of these methods in electrochemical analyte detection. Its detection by voltammetry on carbon electrodes has proved to be more complex due to irreversible slow electron transfer kinetics. Commercial production/availability of simple, easy-to-use measurement devices as portable or pocket-sized analyzers is still challenging sensor technology. Traditional approaches to measure H_2O_2 in vivo suffers with multiple problems: (1) nonspecific probes that react with other reactive oxygen and nitrogen species (2) sensitivity issues related with production of H_2O_2 at low concentration and short half-life (3) rapid diffusion of H_2O_2 across membranes (4) detection of H_2O_2 levels requires deep tissue imaging techniques with high resolution.

Conclusion and future perspectives

This review article addresses the updated summary of electrochemical H_2O_2 biosensor. In conclusion, biosensing methods are better than conventional methods (colorimetry, titration, chromatography, spectrophotometry, fluorimetry, chemiluminescence) for determination of H_2O_2 as they are comparatively simple, sensitive, specific, and rapid and even can work with complete automation. The nanomaterial-based biosensor exhibited better analytical performances in terms of working potential (−0.6–0.45), detection limit (0.00045–340 µM) and sensitivity (0.3 µAmp/mM/cm^2) which was owing to the large surface area, high electrical and optical properties of nanomaterials. Among the electrochemical H_2O_2 biosensor, enzymes and proteins (HRP, catalase and Hb-based biosensors are dominating. The HRP/Hb based H_2O_2 biosensors was upgraded further with the use of nanoparticles of enzymes/proteins. Beside increased surface area protein nanomolecules also exhibit exceptional optical, electronic, mechanical and thermal properties [91]. Hence the future research could be focus on application of protein nanoparticles in construction of highly sensitive H_2O_2 biosensors. Attempt can also be made by designing electronic chip for the laboratory model of H_2O_2 biosensor, which could be used outside the laboratory. The development, optimization and characterization of microsensors can be done to ensure a successful transfer of the technology from in vitro proof of concept to in vivo analysis.

References

1. Vogel AI (1989) Textbook of quantitative chemical analysis, 5th edn. Longman Scientific and Technical, Harlow
2. Jr. WM, Bell H (1966) Titrimetric determination of hydrogen peroxide in alkaline solution. Talanta 13:925–928. https://doi.org/10.1016/0039-9140(66)80189-3
3. Elias H, Vayssié S (2005) Reactive peroxo compounds generated in situ from hydrogen peroxide: kinetics and catalytic application in oxidation processes. Peroxide Chem. https://doi.org/10.1002/3527600396.ch6
4. Lopez-Lazaro M (2007) Hydrogen peroxide. Encycl Cancer. https://doi.org/10.1007/978-3-540-47648-1_2887
5. Conner W (1993) Hydrogen peroxide safety issues. U.S. Department of Energy. https://doi.org/10.2172/10158827
6. Winterbourn CC (2013) The Biological chemistry of hydrogen peroxide. Hydrogen peroxide and cell signaling, part C methods in enzymology 3–25. https://doi.org/10.1016/b978-0-12-405881-1.00001-x
7. Choi H, Cuenca J, Attard G, Porch A (2014) A novel concentration detection method of hydrogen peroxide using microwave cavity perturbation technique. 2014 44th European Microwave Conference. https://doi.org/10.1109/eumc.2014.6986513
8. Hu L, Han S, Liu Z et al (2011) A versatile strategy for electrochemical detection of hydrogen peroxide as well as related enzymes and substrates based on selective hydrogen peroxide-mediated boronate deprotection. Electrochem Commun 13:1536–1538. https://doi.org/10.1016/j.elecom.2011.10.016
9. Guadagnini L, Tonelli D, Giorgetti M (2010) Improved performances of electrodes based on Cu2-loaded copper hexacyanoferrate for hydrogen peroxide detection. Electrochim Acta 55:5036–5039. https://doi.org/10.1016/j.electacta.2010.04.019
10. Giannoudi L, Piletska EV, Piletsky SA (2006) Development of biosensors for the detection of hydrogen

peroxide. Biotechnol Appl Photosynth Proteins. https://doi.org/10.1007/978-0-387-36672-2_16
11. Klassen NV, Marchington D, Mcgowan HC (1994) H_2O_2 determination by the I3-method and by $KMnO_4$ titration. Anal Chem 66:2921–2925. https://doi.org/10.1021/ac00090a020
12. Murty KN, Rao KR, Chalam GK (1981) Potentiometric determination of H_2O_2 and sodium perborate with potassium dichromate. Proc Natl Acad Sci 47:293–95
13. Kieber RJ, Helz GR (1986) Two-method verification of hydrogen peroxide determinations in natural waters. Anal Chem 58:2312–2315. https://doi.org/10.1021/ac00124a043
14. Putt KS, Pugh RB (2013) A high-throughput microtiter plate based method for the determination of peracetic acid and hydrogen peroxide. PLoS One. https://doi.org/10.1371/journal.pone.0079218
15. Zaribafan A, Haghbeen K, Fazli M, Akhondali A (2014) Spectrophotometric method for hydrogen peroxide determination through oxidation of organic dyes. Environ Stud Persian Gulf 1:93–101
16. Matsubara C, Kudo K, Kawashita T, Takamura K (1985) Spectrophotometric determination of hydrogen peroxide with titanium 2-((5-bromopyridyl)azo)-5-(N-propyl-*N*-sulfopropylamino)phenol reagent and its application to the determination of serum glucose using glucose oxidase. Anal Chem 57:1107–1109. https://doi.org/10.1021/ac00283a032
17. Clapp PA, Evans DF, Sheriff TS (1989) Spectrophotometric determination of hydrogen peroxide after extraction with ethyl acetate. Anal Chim Acta 218:331–334. https://doi.org/10.1016/s0003-2670(00)80309-8
18. Mukhopadhyay D, Dasgupta P, Roy DS et al (2016) A sensitive in vitro spectrophotometric hydrogen peroxide scavenging assay using 1,10-phenanthroline. Free Rad Antioxid 6:124–132. https://doi.org/10.5530/fra.2016.1.15
19. Elnemma EM (2004) Spectrophotometric determination of hydrogen peroxide by a hydroquinone-aniline system catalyzed by molybdate. Bull Korean Chem Soc 25:127–129. https://doi.org/10.5012/bkcs.2004.25.1.127
20. Zhang L-S, Wong GT (1994) Spectrophotometric determination of H_2O_2 in marine waters with leuco crystal violet. Talanta 41:2137–2145. https://doi.org/10.1016/0039-9140(94)00199-5
21. Shariati RM, Irandoust M, Salarmand N (2015) Development of a spectrophotometric method for determination of hydrogen peroxide using response surface methodology Austin. J Anal Pharm Chem 2(5):1051
22. Huang Y, Cai R, Mao L et al (1999) Spectrophotometric determination of hydrogen peroxide using BETA-CD-Hemin as a mimetic enzyme of peroxidase. Anal Sci 15:889–894. https://doi.org/10.2116/analsci.15.889
23. Zhang Q, Fu S, Li H, Liu Y (2013) A novel method for the determination of hydrogen peroxide in bleaching effluents by spectroscopy. BioResources. https://doi.org/10.15376/biores.8.3.3699-3705
24. Eisenberg G (1943) Colorimetric determination of hydrogen peroxide. Ind Eng Chem Anal Edn 15:327–328. https://doi.org/10.1021/i560117a011
25. Ernst G, John TP (1980) Method for determination of hydrogen peroxide, with its application illustrated by glucose assay. Clin Chem 26:658–660
26. Pick E, Keisari Y (1980) A simple colorimetric method for the measurement of hydrogen peroxide produced by cells in culture. J Immunol Methods 38:161–170. https://doi.org/10.1016/0022-1759(80)90340-3
27. Fernando CD, Soysa P (2015) Optimized enzymatic colorimetric assay for determination of hydrogen peroxide (H_2O_2) scavenging activity of plant extracts. MethodsX 2:283–291. https://doi.org/10.1016/j.mex.2015.05.001
28. Su G, Wei Y, Guo M (2011) Direct colorimetric detection of hydrogen peroxide using 4-nitrophenyl boronic acid or its pinacol ester. Am J Anal Chem 02:879–884. https://doi.org/10.4236/ajac.2011.28101
29. Nitinaivinij K, Parnklang T, Thammacharoen C et al (2014) Colorimetric determination of hydrogen peroxide by morphological decomposition of silver nanoprisms coupled with chromaticity analysis. Anal Methods 6:9816–9824. https://doi.org/10.1039/c4ay02339k
30. Takahashi A, Hashimoto K, Kumazawa S, Nakayama T (1999) Determination of hydrogen peroxide by high-performance liquid chromatography with a cation-exchange resin gel column and electrochemical detector. Anal Sci 15:481–483. https://doi.org/10.2116/analsci.15.481
31. Wada M, Inoue K, Ihara A et al (2003) Determination of organic peroxides by liquid chromatography with on-line post-column ultraviolet irradiation and peroxyoxalate chemiluminescence detection. J Chromatogr A 987:189–195. https://doi.org/10.1016/s0021-9673(02)01473-5
32. Nepomnyashchikh YV, Borkina GG, Karavaeva AV, Perkel AL (2005) Photometric and gas-chromatographic determination of hydrogen peroxide and peroxybutanoic acid in oxidized butanoic acid. J Anal Chem 60:1024–1028. https://doi.org/10.1007/s10809-005-0231-6
33. Magara K, Ikeda T, Sugimoto T, Hosoya S (2007) Quantitative analysis of hydrogen peroxide by high performance liquid chromatography. Jpn Tappi J 61:1481–1493. https://doi.org/10.2524/jtappij.61.1481
34. Steinberg SM (2012) High-performance liquid chromatography method for determination of hydrogen peroxide in aqueous solution and application to simulated Martian soil and related materials. Environ Monit Assess 185:3749–3757. https://doi.org/10.1007/s10661-012-2825-4
35. Gimeno P, Bousquet C, Lasu N, Maggio AF, Civade C, Breneir C, Lempereur L (2015) High-performance liquid chromatography method for the determination of hydrogen peroxide present or released in teeth bleaching kits and hair cosmetic products. J Pharm Biomed Anal 107:386–393
36. Segawa T, Kamidate T, Watanabe H (1990) Determination of hydrogen peroxide with fluorescein chemiluminescence catalyzed by horseradish peroxidase. Anal Sci 6:763–764. https://doi.org/10.2116/analsci.6.763
37. Tugba TU, Elmas GOK, Serdar A (2003) Determination of H_2O_2 content of various water samples using a chemiluminescence technique. Turk J Chem 27:41
38. Pérez FJ, Rubio S (2006) An improved chemiluminescence method for hydrogen peroxide determination in plant tissues. Plant Growth Regul 48:89–95. https://doi.org/10.1007/s10725-005-5089-y
39. Onoda M, Uchiyama T, Mawatari K-I et al (2006) Simple and rapid determination of hydrogen peroxide using phosphine-based fluorescent reagents with sodium tungstate dihydrate. Anal Sci 22:815–817. https://doi.org/10.2116/analsci.22.815
40. Paital B (2014) A modified fluorimetric method for determination of hydrogen peroxide using homovanillic acid oxidation principle. Biomed Res Int 2014:1–8. https://doi.org/10.1155/2014/342958
41. Chen H, Yu H, Zhou Y, Wang L (2007) Fluorescent quenching method for determination of trace hydrogen peroxide in rain water. Spectrochim Acta Part A Mol Biomol Spectrosc 67:683–686. https://doi.org/10.1016/j.saa.2006.07.057
42. Lee D, Khaja S, Velasquez-Castano JC et al (2007) In vivo imaging of hydrogen peroxide with chemiluminescent nanoparticles. Nat Mater 6:765–769. https://doi.org/10.1038/nmat1983
43. Lee I-J, Hwang O, Yoo D-H et al (2011) Detection of hydrogen peroxide in vitro and in vivo using peroxalate chemiluminescent micelles. Bull Korean Chem Soc 32:2187–2192. https://doi.org/10.5012/bkcs.2011.32.7.2187

44. Jin H, Heller DA, Kalbacova M et al (2010) Detection of single-molecule H_2O_2 signalling from epidermal growth factor receptor using fluorescent single-walled carbon nanotubes. Nat Nanotechnol 5:302–309. https://doi.org/10.1038/nnano.2010.24
45. Kim J-H, Patra CR, Arkalgud JR et al (2011) Single-molecule detection of H_2O_2 mediating angiogenic redox signaling on fluorescent single-walled carbon nanotube array. ACS Nano 5:7848–7857. https://doi.org/10.1021/nn201904t
46. Wei H, Wang E (2008) FE_3O_4 magnetic nanoparticles as peroxidase mimetics and their applications in H_2O_2 and glucose detection. Anal Chem 80:2250–2254. https://doi.org/10.1021/ac702203f
47. Gondran C (2013) Electrochemical biosensors. Chem Sens Biosens. https://doi.org/10.1002/9781118561799.ch13
48. Yunus S, Jonas AM, Lakard B (2013) Potentiometric biosensors. Encycl Biophys. https://doi.org/10.1007/978-3-642-16712-6_714
49. Parrilla M, Canovas R, Andrade FJ (2017) Enhanced potentiometric detection of hydrogen peroxide using a platinum electrode coated with nafion. Electroanalysis 29:223–230
50. Zheng X (2000) Potentiometric determination of hydrogen peroxide at MnO_2-doped carbon paste electrode. Talanta 50:1157–1162. https://doi.org/10.1016/s0039-9140(99)00223-4
51. Punter J, Colomer-Farrarons J, Ll P (2013) Bioelectronics for amperometric biosensors. State of the art in biosensors—general aspects. In: Rinken T (ed) Biomedical engineering. https://doi.org/10.5772/52248 (**ISBN 978-953-51-1004-0**)
52. Sezgintürk MK, Dinçkaya E (2008) H_2O_2 determination by a biosensor based on hemoglobin. Prep Biochem Biotechnol 39:1–10. https://doi.org/10.1080/10826060802589361
53. Kafi AKM, Lee D-Y, Park S-H, Kwon Y-S (2007) A hydrogen peroxide biosensor based on peroxidase activity of hemoglobin in polymeric film. J Nanosci Nanotechnol 7:4005–4008. https://doi.org/10.1166/jnn.2007.095
54. Zhang D, Zhao H, Fan Z et al (2015) A highly sensitive and selective hydrogen peroxide biosensor based on gold nanoparticles and three-dimensional porous carbonized chicken eggshell membrane. Plos One. https://doi.org/10.1371/journal.pone.0130156
55. Yue H, He J, Xiao D, Choi MMF (2013) Biosensor for determination of hydrogen peroxide based on Yucca filamentosa membrane. Anal Methods 5:5437. https://doi.org/10.1039/c3ay40678d
56. Choi MM, Yiu TP (2004) Immobilization of beef liver catalase on eggshell membrane for fabrication of hydrogen peroxide biosensor. Enzyme Microb Technol 34:41–47. https://doi.org/10.1016/j.enzmictec.2003.08.005
57. Shamsipur M, Asgari M, Mousavi MF, Davarkhah R (2011) A novel hydrogen peroxide sensor based on the direct electron transfer of catalase immobilized on nano-sized NiO/MWCNTs composite film. Electroanalysis 24:357–367. https://doi.org/10.1002/elan.201100453
58. He J, Sunarso J, Zhu Y et al (2017) High-performance non-enzymatic perovskite sensor for hydrogen peroxide and glucose electrochemical detection. Sens Actuators B 244:482–491. https://doi.org/10.1016/j.snb.2017.01.012
59. Mutyala S, Mathiyarasu J (2016) A reagentless non-enzymatic hydrogen peroxide sensor presented using electrochemically reduced graphene oxide modified glassy carbon electrode. Mater Sci Eng 69:398–406. https://doi.org/10.1016/j.msec.2016.06.069
60. Paixão TERELEC, Bertotti M (2008) Ruthenium oxide hexacyanoferrate modified electrode for hydrogen peroxide detection. Electroanalysis 20:1671–1677. https://doi.org/10.1002/elan.200804231
61. Kondo T, Tamura A, Fujishima A, Kawai T (2008) High sensitivity electrochemical detection of hydrogen peroxide at a cobalt phthalocyanine-modified boron-doped diamond electrode. ECS Trans. https://doi.org/10.1149/1.2981152
62. Xu X, Zhang J, Guo F et al (2011) A novel amperometric hydrogen peroxide biosensor based on immobilized Hb in pluronic P123-nanographene platelets composite. Coll Surf B 84:427–432. https://doi.org/10.1016/j.colsurfb.2011.01.037
63. Guo F, Xu X, Sun Z et al (2011) A novel amperometric hydrogen peroxide biosensor based on electrospun Hb–collagen composite. Coll Surf B 86:140–145. https://doi.org/10.1016/j.colsurfb.2011.03.032
64. Xu Y, Hu C, Hu S (2008) A hydrogen peroxide biosensor based on direct electrochemistry of hemoglobin in Hb–Ag sol films. Sens Actuators B 130:816–822. https://doi.org/10.1016/j.snb.2007.10.048
65. Gao F, Yuan R, Chai Y et al (2007) Amperometric third-generation hydrogen peroxide biosensor based on immobilization of Hb on gold nanoparticles/cysteine/poly(p-aminobenzene sulfonic acid)-modified platinum disk electrode. Coll Surf A 295:223–227. https://doi.org/10.1016/j.colsurfa.2006.09.006
66. Li J, Mei H, Zheng W et al (2014) A novel hydrogen peroxide biosensor based on hemoglobin–collagen-CNTs composite nanofibers. Coll Surf B 118:77–82. https://doi.org/10.1016/j.colsurfb.2014.03.035
67. Kafi A, Yin F, Shin H-K, Kwon Y-S (2006) Hydrogen peroxide biosensor based on DNA–Hb modified gold electrode. Thin Solid Films 499:420–424. https://doi.org/10.1016/j.tsf.2005.06.073
68. Bai Z, Li G, Liang J et al (2016) Non-enzymatic electrochemical biosensor based on Pt NPs/RGO-CS-Fc nano-hybrids for the detection of hydrogen peroxide in living cells. Biosens Bioelectr 82:185–194. https://doi.org/10.1016/j.bios.2016.04.004
69. Gong Y, Chen X, Lu Y, Yang W (2015) Self-assembled dipeptide–gold nanoparticle hybrid spheres for highly sensitive amperometric hydrogen peroxide biosensors. Biosens Bioelectr 66:392–398. https://doi.org/10.1016/j.bios.2014.11.029
70. Fan Z, Lin Q, Gong P et al (2015) A new enzymatic immobilization carrier based on graphene capsule for hydrogen peroxide biosensors. Electrochim Acta 151:186–194. https://doi.org/10.1016/j.electacta.2014.11.022
71. Chen C, Hong X, Xu T et al (2016) Hydrogen peroxide biosensor based on the immobilization of horseradish peroxidase onto a poly(aniline-co-*N*-methylthionine) film. Synth Met 212:123–130. https://doi.org/10.1016/j.synthmet.2015.12.012
72. Pla-Tolós J, Moliner-Martinez Y, Molins-Legua C, Campins-Falcó P (2016) Colorimetic biosensing dispositive based on reagentless hybrid biocomposite: application to hydrogen peroxide determination. Sens Actuators B 231:837–846. https://doi.org/10.1016/j.snb.2016.03.094
73. Chut SL, Li J, Tan SN (1997) A mediated turnip tissue-based amperometric hydrogen peroxide biosensor. Anal Lett 30:1993–1998. https://doi.org/10.1080/00032719708001715
74. Behera TK, Sahu SC, Satpati B et al (2016) Branched platinum nanostructures on reduced graphene: an excellent transducer for nonenzymatic sensing of hydrogen peroxide and biosensing of xanthine. Electrochim Acta 206:238–245. https://doi.org/10.1016/j.electacta.2016.03.046
75. Kung C-C, Lin P-Y, Buse FJ et al (2014) Preparation and characterization of three dimensional graphene foam supported platinum–ruthenium bimetallic nanocatalysts for hydrogen peroxide based electrochemical biosensors. Biosens Bioelectr 52:1–7. https://doi.org/10.1016/j.bios.2013.08.025
76. Lata S, Batra B, Karwasra N, Pundir CS (2012) An amperometric H_2O_2 biosensor based on cytochrome c immobilized onto nickel oxide nanoparticles/carboxylated multiwalled carbon nanotubes/polyaniline modified gold electrode. Process Biochem 47:992–998. https://doi.org/10.1016/j.procbio.2012.03.018
77. Thenmozhi K, Narayanan SS (2017) Horseradish peroxidase and toluidine blue covalently immobilized leak-free sol–gel composite

biosensor for hydrogen peroxide. Mater Sci Eng 70:223–230. https://doi.org/10.1016/j.msec.2016.08.075
78. Wu Y, Wang F, Lu K et al (2017) Self-assembled dipeptide-graphene nanostructures onto an electrode surface for highly sensitive amperometric hydrogen peroxide biosensors. Sens Actuators B 244:1022–1030. https://doi.org/10.1016/j.snb.2017.01.048
79. Dramińska S, Bilewicz R (2017) Bienzymatic mediatorless sensing of total hydrogen peroxide with catalase and multi-copper enzyme co-adsorbed at carbon nanotube-modified electrodes. Sens Actuators B 248:493–499. https://doi.org/10.1016/j.snb.2017.04.008
80. Tajabadi M, Sookhakian M, Zalnezhad E et al (2016) Electrodeposition of flower-like platinum on electrophoretically grown nitrogen-doped graphene as a highly sensitive electrochemical non-enzymatic biosensor for hydrogen peroxide detection. Appl Surf Sci 386:418–426. https://doi.org/10.1016/j.apsusc.2016.06.045
81. Boujakhrout A, Díez P, Sánchez A et al (2016) Gold nanoparticles-decorated silver-bipyridine nanobelts for the construction of mediatorless hydrogen peroxide biosensor. J Coll Interface Sci 482:105–111. https://doi.org/10.1016/j.jcis.2016.07.074
82. Peng Z, Jiang Z, Huang X, Li Y (2016) A novel electrochemical sensor of tryptophan based on silver nanoparticles/metal-organic framework composite modified glassy carbon electrode. RSC Adv 6:13742–13748. https://doi.org/10.1039/c5ra25251b
83. Liu J, Bo X, Yang J et al (2017) One-step synthesis of porphyrinic iron-based metal-organic framework/ordered mesoporous carbon for electrochemical detection of hydrogen peroxide in living cells. Sens Actuators B 248:207–213. https://doi.org/10.1016/j.snb.2017.03.117
84. Benvidi A, Nafar MT, Jahanbani S et al (2017) Developing an electrochemical sensor based on a carbon paste electrode modified with nano-composite of reduced graphene oxide and $CuFe_2O_4$ nanoparticles for determination of hydrogen peroxide. Mater Sci Eng 75:1435–1447. https://doi.org/10.1016/j.msec.2017.03.062
85. Zhao W, Jin J, Wu H et al (2017) Electrochemical hydrogen peroxide sensor based on carbon supported Cu@Pt core-shell nanoparticles. Mater Sci Eng 78:185–190
86. Liu F, Bing T, Shangguan D et al (2016) Ratiometric fluorescent biosensing of hydrogen peroxide and hydroxyl radical in living cells with lysozyme–silver nanoclusters: lysozyme as stabilizing ligand and fluorescence signal unit. Anal Chem 88:10631–10638. https://doi.org/10.1021/acs.analchem.6b02995
87. Luo M, Wang W, Zhao Q, Li M, Chen Y, Lu Z, Liu K, Wang D (2017) Chemiluminescence biosensor for hydrogen peroxide determination by immobilizing horseradish peroxidase onto PVA-co-PE nanofiber membrane. Eur Polym J. https://doi.org/10.1016/j.eurpolymj.2017.04.018
88. Manikandan M, Dhanuskodi S, Maheswari N, Muralidharan G, Revathi C, Kumar RR, Rao GM (2017) High performance supercapacitor and non-enzymatic hydrogen peroxide sensor based on tellurium nanoparticles. Sens Bio Sens Res 13:40–48. https://doi.org/10.1016/j.sbsr.2017.02.001
89. Cai B, Zhao M, Wang Y, Zhou Y, Cai H, Ye Z, Huang J (2014) A perovskite-type $KNbO_3$ nanoneedles based biosensor for direct electrochemistry of hydrogen peroxide. Ceram Int 40:8111–8116. https://doi.org/10.1016/j.ceramint.2014.01.005
90. Narwal V, Yadav N, Thakur M, Pundir CS (2017) An amperometric H_2O_2 biosensor based on hemoglobin nanoparticles immobilized on to a gold electrode. Biosci Rep. https://doi.org/10.1042/bsr20170194
91. Narwal V, Pundir C (2017) An improved amperometric triglyceride biosensor based on co-immobilization of nanoparticles of lipase, glycerol kinase and glycerol 3-phosphate oxidase onto pencil graphite electrode. Enzyme Microb Technol 100:11–16. https://doi.org/10.1016/j.enzmictec.2017.01.009